FIRST-GENERATION INTERFEROMETRIC GRAVITATIONAL-WAVE DETECTORS

H. GROTE*, D. H. REITZE+

*MPI for Grav. Physics (AEI), and Leibniz University Hannover, 38 Callinstr., 30167 Hannover, Germany
E-mail: hartmut.grote@aei.mpg.de

+ Physics Department, University of Florida, Gainesville, FL 32611, USA
E-mail: reitze@phys.ufl.edu

In this proceeding, we review some of the basic working principles and building blocks of laser-interferometric gravitational-wave detectors on the ground. We look at similarities and differences between the instruments called GEO, LIGO. TAMA, and Virgo. which are currently (or have been) operating over roughly one decade, and we highlight some astrophysical results to date.

1 Introduction

The first searches for gravitational waves began in earnest 50 years ago with the experiments of Joseph Weber using resonant mass detectors ('Weber Bars'). [1] Weber's pioneering efforts were ultimately judged as unsuccessful regarding the detection of gravitational waves, but from those beginnings interest in gravitational wave detection has grown enormously. For some decades after, a number of resonant mass detectors were built and operated around the globe with sensitivities far greater than those at Weber's time. Some resonant bars are still in operation, but even their enhanced sensitivities today are lower and restricted to a much smaller bandwidth than those of the current laser interferometers.

Over the past decade, km-class ground-based interferometers have been operating in the United States, Italy and Germany, as well as a 300 m arm length interferometer in Japan. Upgrades are underway to second generation configurations with far greater sensitivities. With further astrophysics 'reach', these detectors will usher in the era of gravitational wave astronomy with the expectation of tens or possibly hundreds of events per year based on current rate estimates. [2] (See also the contributions about *Advanced* detectors in this volume.)

Section 2 of this paper presents a brief introduction to ground-based gravitational wave interferometry, detector architecture, and methods used to minimize the influence of external perturbations. Section 3 surveys the currently operational (or operational until late 2010) interferometers, with a particular view on some unique features of the individual instruments. Finally we give a brief review of the most significant observational results to date in Section 4. Parts of this paper have been published as proceeding of the 12th Marcel Grossmann meeting. [3]

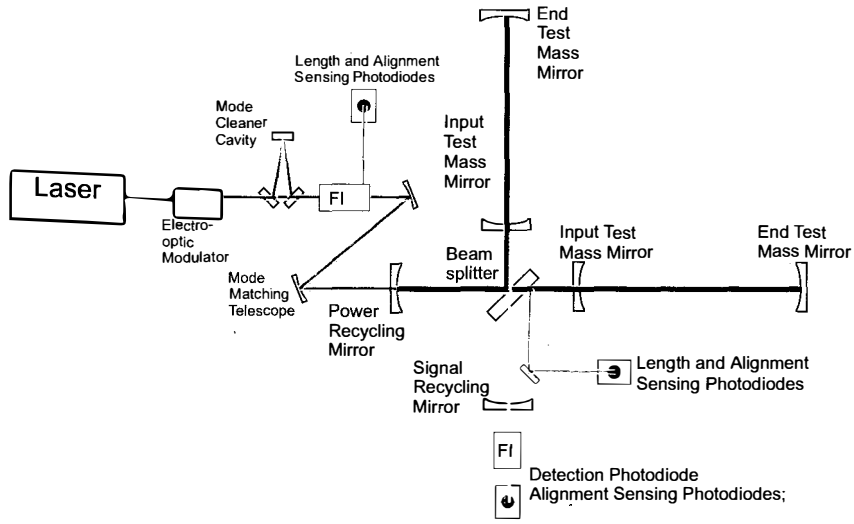

Figure 1: Generic layout example of a ground-based laser-interferometric gravitational-wave detector. The basic building blocks are a laser, input optics (mode cleaner cavity, Faraday Isolator FI, mode matching telescope), and a Michelson interferometer consisting of a beam splitter and two end test mass mirrors. Additional optics are: Power recycling mirror, to resonantly enhance the circulating light power, Input test mass mirrors, to increase the light storage time in the long arms, a signal recycling mirror to increase and optimize gravitational-wave signal storage time. First-generation interferometers around the globe only use subsets of these optics, as detailed in the text. Length- and alignment sensing photodiodes are shown, together with the detection photodiode at the output port of the Michelson interferometer (or the signal recycling cavity, respectively).

2 Principles of ground-based Gravitational Wave Interferometers

Gravitational waves are strains, or changes in length per unit length, $\Delta L/L$, which come about due to the time dependence of the quadrupole mass moment, $I_{\mu\nu}(t)$, of massive objects. From a practical standpoint, astrophysical objects moving at relativistic speeds are needed to generate gravitational waves of sufficient amplitude to enable detection by earth-based interferometers. Several excellent references exist which describe gravitational waves and their intimate connection with astrophysics (see, for example, Ref.[4] and Ref.[5] and references therein). In this section, we briefly describe the generic workings of laser-interferometric gravitational wave detectors.

Figure 1 displays the most general layout of a ground-based interferometer. A frequency- and amplitude-stabilized laser is phase-modulated via electro-optic modulation and injected into a mode-cleaner triangular optical cavity to provide an additional level of frequency and amplitude stabilization as well as to suppress pointing fluctuations of the input laser beam. The mirrors in the mode cleaner cavity and all subsequent mirrors comprising the interferometer are isolated from low-frequency ground motion by seismic isolation platforms and mirror suspensions (see section 2.1). From the mode-cleaner, the beam passes through a Faraday isolator (FI) which functions somewhat analogously to an optical 'diode', diverting back-reflections from the interferometer to length and alignment sensing photodiodes and preventing the light from entering the mode-cleaner. The FI is followed by a beam-expanding telescope which mode-matches the input laser mode into the interferometer cavity mode.

The basis for the interferometer architecture is a Michelson interferometer, consisting of a beam splitter and the two end test mass mirrors, and a detection photodiode. A second FI can be used to prevent light scattering from the photodiode back into the interferometer. To

minimize noise associated with amplitude fluctuations of the laser, the interferometer differential path length is set to interfere carrier light destructively at the detection photodiode such that the quiescent state is nearly dark. A passing gravitational wave differentially modulates the round-trip travel time of the light in the arms at the gravitational wave frequency which in turn modulates the light intensity at the detection photodiode. In effect, the interferometer transduces the dynamic metric perturbation imposed by the passing gravitational wave to photocurrent in the detection photodiode. The magnitude of photocurrent depends not only on the amplitude, but also on the direction and polarization of the passing gravitational wave.

Beyond the simple Michelson configuration, the sensitivity of the interferometer can be further increased in three ways. By adding input test mass mirrors into each arm, Fabry-Perot cavities are formed, effectively increasing the light storage time in the arms (or, in an alternative view, amplifying the phase shift for a given amount of displacement). Second, since the recombined laser light at the beam splitter interferes constructively toward the laser, it can be coherently recirculated back into the interferometer by a 'power-recycling' mirror located in between the mode-matching telescope and the beam splitter. Finally, the gravitational signal itself can be recycled by placing a 'signal-recycling' mirror between the beam splitter and the detection photodiode to recirculate the light modulated by the gravitational wave into the interferometer, further increasing the light storage time and thus the depth of modulation by the gravitational wave. The signal-recycling mirror also allows for tuning of the response curve of the interferometer. By shifting the signal-recycling mirror a fraction of a wavelength from resonant recirculation ('tuned' operation), specific frequencies of the light are resonantly recycled at the expense of others ('detuned' operation), allowing for enhanced sensitivities over specific frequency ranges of interest.

Current interferometers are designed to be sensitive in the frequency range from approximately 10-50 Hz out to a few kHz. Fundamental noises limiting interferometer sensitivity depend on the specifics of the interferometer design, and different interferometers have approached the task of minimizing interferometer noise in different ways. However, the limiting sensitivity envelope for all ground-based detectors roughly breaks down as follows: seismic ground motion at low frequencies, thermal noise due to the Brownian motion of the mirror suspension wires and mirror coatings in the mid-frequency bands, and shot noise at high frequencies. In addition, technical noise sources from length and alignment sensing and control systems can also limit interferometer performance, in particular at the low-frequency. end. To minimize phase noise from light scattering off molecules, the components of the interferometer and the input optics (mode-cleaner, FI, and telescope) are located in an ultrahigh vacuum system. Light scattering off mirrors however, which can be reflected by seismically 'noisy' components and then being re-directed to interfere with the main interferometer beams, can also contribute to excess noise.

2.1 Seismic isolation and suspensions

A typical ambient horizontal ground motion on the surface of the earth is about $10^{-10}\,\mathrm{m}/\sqrt{\mathrm{Hz}}$ at 50 Hz. Depending on the choice of sensitive frequency band, the test mass mirrors of gravitational-wave interferometers have to be quieter by roughly 10 orders of magnitude at these frequencies, motivating sophisticated seismic isolation systems.

The principle used to isolate optical components such as mirrors from ground motion is to suspend the components as pendulums, making use of the attenuation provided by the pendulums displacement transfer function above the fundamental pendulum resonance frequency. Most of the projects to date use cascaded multiple-pendulum chains, in order to increase the amount of attenuation. Figure 2 shows two examples of cascaded pendulums as in use in Virgo and GEO 600 (see section 3 below, for the individual projects), namely a), the Virgo 'super attenuator', and b), the GEO 600 suspension.

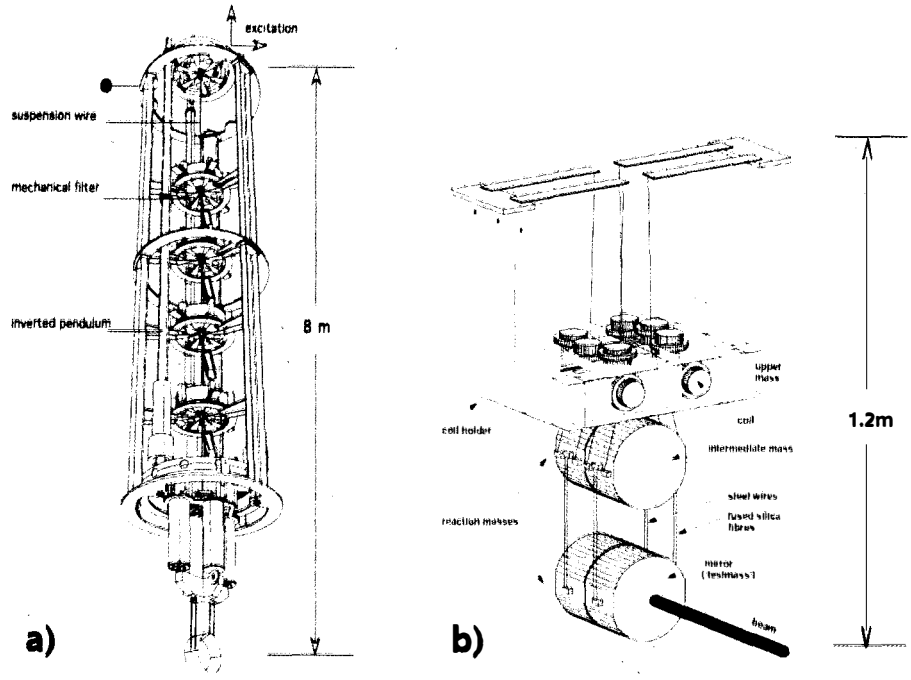

Figure 2: a) The Virgo 'super attenuator' consists of multiple pendulum stages connected by single suspension wires. Vertical isolation is provided by the 'mechanical filter' stages, which act as pendulum masses, but also hold the subsequent suspension wire by blade-springs. b) The GEO 600 suspension consists of 3 pendulum stages (including the test-mass mirror). The upper two stages provide vertical isolation by steel springs holding the suspension wires. Both suspension types a) and b) use fused silica fibres to suspend the test mass mirror from the penultimate, or intermediate mass.

A Virgo super-attenuator [6] consists of multiple pendulum stages, which are connected to each other by single suspension wires. In addition to the inherent horizontal isolation of the pendulums, the intermediate pendulum masses, denoted as *mechanical filters,* provide vertical isolation by a *magnetic anti-spring* mechanism. The penultimate mass holds the test-mass mirror on 4 suspension slings, such that angular control can be applied to the mirror from the penultimate mass. In addition to this, angular and longitudinal control forces can be applied to the mirror by a reaction mass (not shown in Figure 2), suspended around the test mass. Coils are attached to the reaction mass, applying forces to magnets glued onto the test mass. The mechanical filter at the top of the suspension chain is supported by an inverted pendulum, completing the supreme low-frequency passive isolation of the super-attenuator. Active feedback control using position- and inertia sensors is required to keep the inverted pendulum at its operating point. The GEO suspension is much more compact in total dimensions, and makes use of three cascaded pendulum stages. Vertical isolation is provided by blade springs, holding the suspension wires of the first and second pendulum stage. For two of the main test masses GEO uses two similar pendulum chains closely located to each other, as shown in Figure 2. The second pendulum chain serves as a reaction 'platform' from which forces can be applied to the test-mass chain without using force actuators referenced to the much larger ground motion.

2.2 *Control*

While suspended optics are supremely quiet in the measurement band of interest (i.e. above 10-50 Hz) the motion of the suspended optics is resonantly enhanced on the eigenmodes of the suspensions, typically around 0.5 to a few Hz. Therefore, different techniques are employed to reduce motion amplitudes of these modes. In many cases, actual mirror motion is measured locally by shadow-sensors, CCD images, or optical lever configurations. Feedback is then applied by coil/magnet actuators to damp the motion of pendulum components. This type of damping can be applied at different levels of the suspension chain, preferably on one of the upper masses to reduce re-introduced displacement noise in the measurement band.

To achieve the sensitivities required for gravitational wave detection, all of the interferometer mirrors must be held to absolute positions of a picometer or less in the presence of several sources of displacement noise. Global length sensing and control systems keep the cavities locked on resonance, using sophisticated variants of the Pound-Drever-Hall cavity locking technique. Phase modulation by the electro-optic modulator (see Figure 1) produces radio-frequency (RF) sidebands on the laser light which serve as references (local oscillators) for sensing length changes in the various length degrees of freedom. In addition, the alignment of the mirrors must be maintained to a few nanoradians using a sensing and control system based on a spatial analog of Pound-Drever-Hall locking.

Hundreds of control loops are thus necessary to keep the interferometer at its nominal operating point. The procedure of bringing the interferometer to this highly-controlled state is non-trivial, and all of the projects have spent many months to years to arrive at reliably reproducible locking sequences, which have become highly automated in most cases.

3 First generation Detectors around the Globe

At the present time, there are five gravitational wave observatories — two LIGO sites in the US, the Virgo and GEO 600 sites in Europe, and the TAMA 300 observatory in Japan (see Figure 3). These observatories have been in operation for the past decade, and constitute the first generation of large-scale interferometers. In this sense the term 'first generation' refers to the time at which these instruments have been built and are operating. However, as we will see below, some of the instruments employ techniques which are technically more advanced than others. These techniques are commonly described as 'second generation' or 'advanced' techniques, with the anticipation that they will be widely implemented in the detector generations planned to replace the existing ones. On these planned upgrades (see other papers in this volume) the infrastructures including buildings, vacuum systems etc. will be re-used, but substantial parts of the interferometer will be replaced with new systems.

3.1 *LIGO*

LIGO consists of two separately located facilities in the United States, one in Hanford, Washington and one in Livingston, Louisiana. The LIGO Hanford Observatory used to house two interferometers, a 4–km arm length interferometer and a 2–km arm length interferometer. The LIGO Livingston Observatory houses a single 4–km long interferometer. The 2–km interferometer in Hanford was taken out of operation in summer 2009, and the two 4–km interferometers were taken out of operation in October 2010, to make way for the *Advanced LIGO* project (see article on Advanced LIGO in this volume). Here we report on the LIGO interferometers up to October 2010, referred to as *Initial* and *Enhanced* LIGO.

The three initial LIGO interferometers were identical in configuration, employing Fabry-Perot arm cavities and power-recycling (but not signal recycling). The seismic isolation system of initial LIGO consisted of passive pre-isolation stacks, using alternating layers of metal and

Figure 3: Global map showing the locations of the first-generation laser-interferometric gravitational wave detectors: The LIGO interferometers in the US, the GEO 600 interferometer in Germany, the Virgo interferometer in Italy, and the TAMA 300 interferometer in Japan.

constrained-layer damped metal coil springs in fluoro-elastomer seats. The test masses were suspended as single-stage pendulums with the suspension point of the pendulums being pre-isolated by the passive spring/metal stacks. At the Livingston site, the higher environmental (mainly anthropogenic) seismic noise made it necessary to install an additional active seismic pre-isolation stage, making use of hydraulic actuators which move the bases of the spring/metal stacks, to counteract seismic motion. [7]

While conservative in the suspension design, the two LIGO 4–km interferometers have been leading in peak sensitivity, as well as over most of the frequency spectrum, with peak strain sensitivities of approximately 2 x $10^{-23}/\sqrt{Hz}$ in the 150–200 Hz region. (See Figure 4 for the strain sensitivities of the three LIGO interferometers during the S5 science run.) An alternative way of characterizing interferometer sensitivity comes from considering how far a specific astrophysical source can be detected. A typical measure of this kind is the range as the distance to which an interferometer can detect the last few moments of orbital decay (inspiral) and merger of a 1.4–1.4 M_{sun} (solar mass) binary neutron star system (for non-spinning neutron stars) with a signal-to-noise ratio of 8. If an optimal orientation of the orbital plane of the neutron stars with respect to the interferometer is assumed, the LIGO interferometers were capable of detecting 1.4–1.4 M_{sun} binary neutron star coalescences out to approximately 35 Mpc during the S5 science run.

In the years from 2007 to 2009, the two 4–km instruments were partially upgraded (within the *enhanced* LIGO project) to moderately increase their sensitivity and to test techniques, to be used in the advanced LIGO project. The most important of these upgrades comprised:

- installation of a more powerful main laser, increasing the available power at the input modecleaner from approx. 10 to 30 W, and the replacement of electro-optic modulators and Faraday isolators to handle the increased power with out distorting the laser beam.

- upgrade of the thermal compensation system, required to compensate for optical distor-

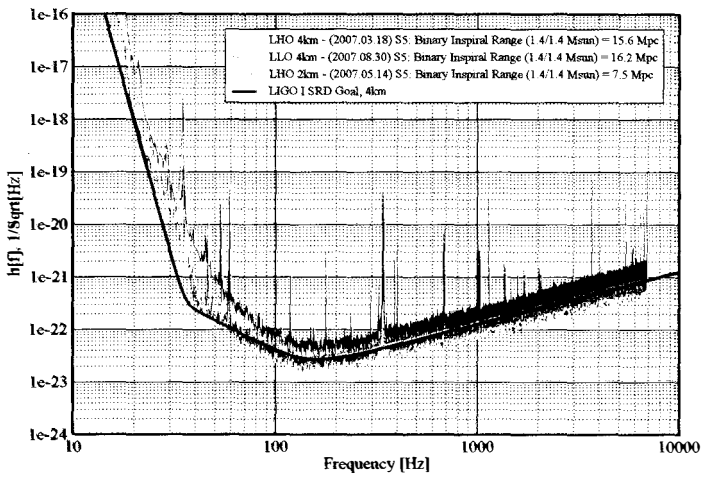

Figure 4: Representative strain sensitivities of the three LIGO interferometers during LIGO's S5 science run. The binary inspiral ranges are here given for an average orientation of the source with respect to the detector.

tions of the laser beams, caused by the high utilized laser power.

- the transition from heterodyne to homodyne readout of the gravitational-wave signal, and the installation of an output-mode cleaner (an additional optical resonator in the output beam) compatible with homodyne readout.

The achieved sensitivities of the two 4–km LIGO instruments up to their end of operation were factors of about 1.4-1.6 better in the high-frequency region above several 100 Hz, compared to the sensitivities shown in Figure 4. The range to detect binary neutron star coalescences was increased from 35 Mpc to about 50 Mpc for an optimal orientation of the source.

A much more detailed overview of the LIGO interferometers can be found in Ref. [8].

3.2 Virgo

The Virgo interferometer located in Cascina, Italy (near Pisa), is operated by a joint consortium of Italian, French, Dutch, Polish, and Hungarian scientists.[9,10] The Virgo interferometer topology is identical to that of the LIGO interferometers, consisting of power-recycling and employing Fabry-Perot arm cavities. The Virgo arms are 3 km in length. A very distinct difference to LIGO is the use of the 'super-attenuator' as seismic isolation system, as described in section 2.1.

As a result of the sophisticated low-frequency isolation, the Virgo interferometer possesses the best strain sensitivity in the low 10–40 Hz band. Virgo was designed to be slightly less sensitive than the LIGO 4 km interferometers in the 40–1000 Hz band, and comparably sensitive above 1 kHz. The Virgo interferometer also enjoys a higher duty cycle than LIGO due to its enhanced seismic isolation, which allows allocation of required actuation forces along different points in the suspension chain. Virgo strain sensitivity curves are shown in Figure 5.

Virgo conducted its first long-duration science run (designated VSR1) during the period May - October 2007. Virgo and LIGO entered into a data sharing agreement prior to the VSR1 run, joining the LIGO and GEO 600 interferometers; since May 2007, Virgo, LIGO, and GEO 600 have been conducting joint science runs and coordinated run planning. Upon

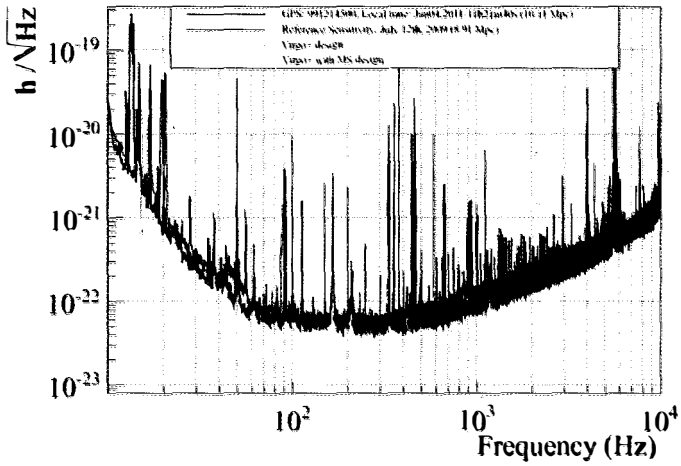

Figure 5: Representative strain sensitivities of Virgo, as of July 2009 and June 2011 (VSR4). In the period after 2009, monolithic suspensions were implemented and the finesse of the arm cavities was increased. The sensitivity to binary neutron star inspirals is about 10 Mpsec for average source orientation. Due to its unique low-frequency sensitivity Virgo achieves a range of more than 70 Mpc for 100–100 M_{sun} black-hole binary systems with an average source orientation.

completion of VSR1, Virgo entered into a period of upgrades to improve detector sensitivity and test advanced techniques. In 2009/2010 Virgo has implemented monolithic fibre suspensions [11] directly bonded to the mirrors, to lower thermal noise. Further, the finesse of the Fabry-Perot arms was increased and thermal compensation systems for radius-of-curvature adjustment were implemented, in order to optimally match the radii-of curvature of the test masses. A science run together with the GEO 600 detector has started on 3rd June 2011 (VSR4/S6e), and is scheduled to last 3 months. After this period, Virgo is starting the advanced Virgo project (see contribution about advanced Virgo in this volume).

3.3 GEO 600

GEO 600[12] is a British-German project located 20 km south of Hannover, Germany. The detector has arm lengths of 600 m and consists of a Michelson interferometer with power- and signal recycling. GEO 600 has no Fabry-Perot cavities in the arms, but once folded arms, resulting in an effective arm length of 1.2 km. GEO uses triple suspensions as described in section 2.1, and the final stage uses fused silica fibres [13] since 2001. GEO is the only project to use electro-static drives to actuate on the main test masses. Other actuation points using coil/magnet actuators are located at the intermediate mass level and at the upper mass level (see Figure 2 b) for the suspension stages). Like for the super-attenuator, this arrangement allows for actuation at different points in the suspension chain, and is a key element for a robust locking of the interferometer. The GEO detector is highly automated and achieved a high duty cycle in the 24/7 run mode of S5 of more than 90 %.

The initial GEO detector was operational until summer 2009, when an upgrade program called *GEO-HF* started. The GEO-HF upgrade focuses on techniques to increase the shot-noise limited sensitivity of GEO. Yet, noise reduction at frequencies below 500 Hz will be done to potentially reach the thermal noise limit of dielectric test-mass coatings. The main points of the

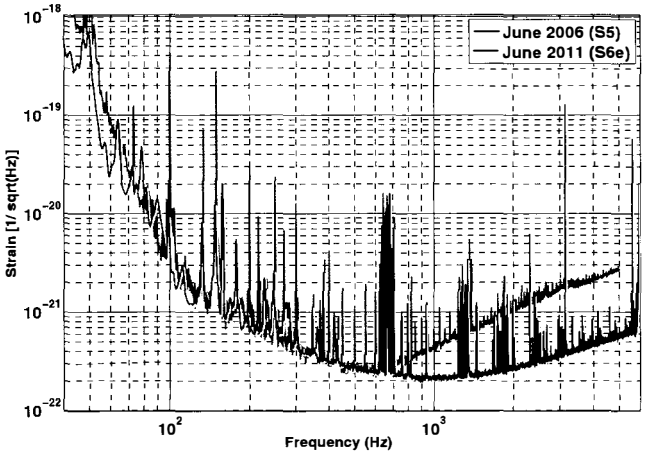

Figure 6: Representative strain sensitivities of the GEO 600 detector. During the fifth science run of the LSC (S5), GEO has been operating with a peak sensitivity around 500Hz, where the signal recycling cavity was tuned to have maximal signal enhancement. Since 2009, GEO operates signal recycling with maximal sensitivity at 'DC' and since 2010 with a higher signal-recycling bandwidth. Together with other improvements, this resulted in a higher sensitivity in the shot-noise limited region above approx. 500 Hz, as shown by the trace from June 2011 (S6c).

GEO-HF upgrade comprise (see also[14]):

- the transition from heterodyne readout to homodyne readout for the gravitational-wave signal, and the installation of an output-mode cleaner compatible with homodyne readout.
- transition from the *detuned* signal recycling, having the peak sensitivity around 500 Hz to *tuned* signal recycling with the peak (shot-noise limited) sensitivity at 'DC'. This goes together with an increase of bandwidth of the signal recycling cavity from about 200Hz to 1 kHz.
- installation of a more powerful main laser, and change of some input optics to accommodate an increased laser power of up to 25 W incident onto the main interferometer.
- injection of squeezed vacuum into the output port of GEO 600, to lower the shot noise.[15,16]

Figure 6 shows strain sensitivities of GEO 600 from 2006 (during the S5 science run) and from 2011, after the GEO-HF upgrade had been under way since about 2 years. GEO now reaches a strain sensitivity of $2 * 10^{-22}/\sqrt{\text{Hz}}$ around 1 kHz, and is comparable sensitive to the Virgo detector at higher frequencies.

3.4 Tama 300

TAMA 300 is a 300 m arm length interferometer located near Tokyo, Japan and is operated by a consortium of Japanese scientists. TAMA 300 employs a Fabry-Perot arm cavity power-recycled Michelson architecture similar to LIGO and Virgo. Although not as sensitive as other large-scale interferometers in operation today, TAMA 300 was the first interferometer to conduct a science

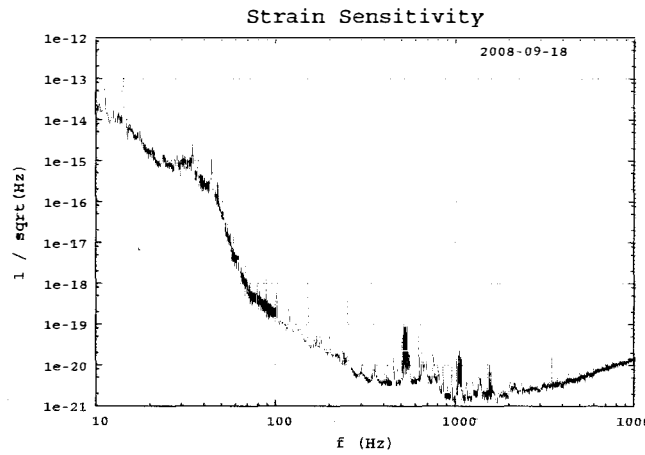

Figure 7: Strain sensitivity of TAMA 300 as of September 2008.

run (August 1999) and has completed eight science runs in the 1999–2004 time frame, with over 1000 hours of accumulated data.

In recent years, TAMA has undergone an extended period of upgrades. TAMA 300's location within a major metropolitan area subjects the interferometer to large amounts of seismic noise. Thus, a two-stage active seismic attenuator system has been developed to mitigate ground noise coupling to the interferometer. [17] Because of its short arm length and high level of seismic disturbance, TAMA 300 is most sensitive in the 1–1.5 kHz band, achieving a strain sensitivity approaching $10^{-21}/\sqrt{Hz}$. The TAMA 300 strain sensitivity curve as of September 2008 is shown in Figure 7. Experience from operating TAMA is utilized in the design of the Large Cryogenic Gravitational-Wave Observatory LCGT in Japan (see contribution in this volume).

4 Astrophysics with the Global Network

Ground-based interferometers have been actively searching for gravitational wave emission from different astrophysical sources for almost a decade. Searches are classified broadly along four types of sources: i) compact binary systems (inspiral, merger, and ring-down), ii) continuously emitting systems (rapidly spinning neutron stars), iii) stochastic sources (noise, eg, the primordial gravitational wave background), and iv) 'burst' sources whose waveforms are unknown or poorly modeled. Analysis methods and algorithms are specifically tailored to each source class. The first observational results on searches for inspiraling compact binaries were published by the TAMA collaboration. [18] A thorough review of recent gravitational wave observational results can be found in Ref. [8]. Here, we simply present a few highlights from recent papers.

4.1 GRB 070201

Gamma ray bursts (GRBs) are intensely bright emissions of γ-rays arising from compact objects, primarily observed at cosmological distances. Most of the observed short hard GRBs are thought to have binary black hole-black hole (BH-BH), black hole-neutron star (BH-NS), or neutron star-neutron star (NS-NS) mergers as their progenitors, although no definitive experimental evidence exists to associate short hard GRBs with binary mergers. The simultaneous observation of a GRB and gravitational wave signal would provide confirmation that binary mergers are a source

f GRBs.

GRB 070201 was an exceptionally short hard GRB observed in the x-ray spectrum by satellites in the Interplanetary Network (IPN). The error box had significant overlap with the M31 Andromeda) galaxy (located 730 kpc from the Milky Way galaxy), thus making it a prime candidate for gravitational wave searches. Data from the LIGO Hanford detectors were analyzed in a 180 s time window around GRB 070201 using both template-based searches for binary mergers and burst search algorithms.[19] No signal was found, and LIGO was able to exclude a compact binary BH-NS, NS-NS merger progenitor of GRB 070201 located in M31 at $> 99\%$ and 90% confidence levels, respectively. The analysis did not rule out a soft gamma repeater (SGR) in M31, but was able to place a limit on energy conversion to gravitational wave of less than 4 x 10^{-4} M_{sun}.

4.2 *Beating the Spindown Limit on the Crab Pulsar*

Spinning neutron stars can emit gravitational waves if they possess ellipticities arising from crustal deformations, internal hydrodynamic modes, or free precession ('wobble'). Ground-based gravitational wave detectors are potentially sensitive to gravitational wave emissions from neutron stars in our galaxy. The Crab pulsar (PSRB0531+21, PSRJ0534+2200), located 2 kpc distant, is a particularly appealing candidate for gravitational wave emission because it is relatively young and rapidly slowing in rotation ('spinning down'). While the predominant energy dissipation mechanisms are magnetic dipole radiation or charged particle emission in the pulsar's magnetosphere, the measured braking index of the Crab pulsar suggests that neither dipole radiation or particle ejection can account for the rotational braking.

Using a subset of data from LIGO's S5 science run, the LIGO Scientific Collaboration searched for gravitational wave emission from the Crab pulsar during a nine month duration during which no pulsar timing jumps occurred.[20] No gravitational waves were observed, and the data was used to set upper limits on the strain $h = 3.35 \times 10^{-25}$ and ellipticity $\epsilon = 1.79 \times 10^{-4}$. The limit on strain is significant in that it implies no more than 5.5% of the energy emitted by the Crab pulsar is in the form of gravitational waves. An updated analysis by the LIGO and Virgo collaborations using a more extensive data set have reduce the upper limit on radiated gravitational wave energy to approximately 2%.[21]

4.3 *The Primordial Gravitational Wave Background*

A stochastic gravitational wave background could arise from an incoherent superposition of point source emitters or from the remnant gravitational wave emission from the Big Bang. Electromagnetic observations of the cosmic microwave background have provided the best knowledge so far of the early universe, however they are limited to probe the universe after the recombination era when the universe became transparent to electromagnetic radiation. Searches for primordial gravitational waves are thus particularly significant from a cosmological standpoint since they directly probe the universe at its earliest epoch.

Recent results by the LIGO Scientific and Virgo Collaborations have placed the most stringent direct observational limit on a stochastic gravitational wave background from the primordial universe. By cross-correlating data from the LIGO Livingston and Hanford 4-km interferometers during the S5 science run, an upper limit of $\Omega_{0,GW} < 6.9 \times 10^{-6}$ on the energy density of stochastic gravitational waves (normalized to the closure energy density of the universe) assuming the gravitational wave background is confined within the 50–150 Hz frequency band.[22] This limit is the best experimental limit in the LIGO frequency band, beating the limit inferred from the Big Bang Nucleosynthesis by almost a factor of 2.

Acknowledgments

The authors gratefully acknowledge support from the Science and Technology Facilities Council (STFC), the University of Glasgow in the UK, the Bundesministerium für Bildung und Forschung (BMBF) and the state of Lower Saxony in Germany. We further gratefully acknowledge the support of the US National Science Foundation through grants PHY-0855313 and PHY-0757968. We also thank Francesco Fidecaro, David Shoemaker, Giovanni Losurdo, and Daisuke Tatsumi for very useful discussions and for supplying material for this article.

References

1. J. Weber, *Phys. Rev.* **117**, 306 (1960).
2. J. Abadie, et al., arXiv:1003.2480 (submitted).
3. D. Reitze, WSPC proceedings MG12, (2010)
4. P. Saulson, *Fundamentals of Interferometric Gravitational Wave Detectors*, 1st edn. (World Scientific Publishing, Hackensack, NJ, 1994).
5. M. Maggiore, *Gravitational Waves: Volume 1: Theory and Experiments*, 1st edn. (Oxford University Press, Oxford, UK, 2007).
6. G. Ballardin, et al., *Rev. Sci. Instrum.* **72**, 3643 (2001).
7. http://etd.lsu.edu/docs/available/etd-01212009-101352/unrestricted/Wen_diss.pdf
8. B. Abbott, et al. (LIGO Science Collaboration), Rep. Prog. Phys. **72**, 076901 (2009).
9. T Accadia and B L Swinkels (for the Virgo Collaboration), Class. Quantum Grav. **27**, 084002 (2010).
10. Information about Virgo can be found at www.virgo.infn.it.
11. M Lorenzini (on behalf of the Virgo Collaboration), Class. Quantum Grav. **27**, 084021 (2010).
12. H Grote (for the LIGO Scientific Collaboration), Class. Quantum Grav. **27**, 084003 (2010).
13. M. V. Plissi, C. I. Torrie, M. E. Husman, N. A. Robertson, K. A. Strain, H. Ward, H. Lück, and J. Hough, *Rev. Sci. Instrum.* **71**, 2539 (2000).
14. H Lück, et al., J. Phys.: Conf. Ser. 228, 012012 (2010).
15. H Vahlbruch, Alexander Khalaidovski, Nico Lastzka, Christian Gräf, Karsten Danzmann, and Roman Schnabel, Class. Quantum Grav. **27**, 084027 (2010).
16. R Schnabel, N Mavalvala, D E McClelland, P K Lam, Nat. Commun. 1:121 doi: 10.1038/ncomms1122 (2010).
17. R Takahashi, K Arai, D Tatsumi, M Fukushima, T Yamazaki, M-K Fujimoto, K Agatsuma, Y Arase, N Nakagawa, A Takamori, K Tsubono, R DeSalvo, A Bertolini, S Marka, and V Sannibale (TAMA Collaboration), *Class. Quantum Grav.* **25**, 114036 (2008).
18. H. Tagoshi, et al., (TAMA Collaboration) *Phys. Rev. D* **63**, 062001 (2001).
19. B. Abbott, et al. (LIGO Science Collaboration), *Astrophys. J.* **681**, 1419 (2008).
20. B. Abbott, et al. (LIGO Science Collaboration), *Astrophys. J. Lett.* **683**, L45 (2008).
21. B. Abbott, et al. (LIGO Science Collaboration), *Astrophys. J.* **713**, 671-685 (2010).
22. B. Abbott, et al. (LIGO Science Collaboration), *Nature* **460**, 990 (2009).

2.
Data analysis: Searches